Molecular Biology of the Cell
Vol. 18, 2904–2911, August 2007

Acetylcholinesterase Mobility and Stability at the Neuromuscular Junction of Living Mice

Isabel Martinez-Pena y Valenzuela and Mohammed Akaaboune

Department of Molecular, Cellular, and Developmental Biology, and Neuroscience Program, University of Michigan, Ann Arbor, MI 48109

Submitted February 2, 2007; Revised April 9, 2007; Accepted May 17, 2007
Monitoring Editor: Tom U. Martin

Acetylcholinesterase (AChE) is an enzyme that terminates acetylcholine neurotransmitter function at the synaptic cleft of cholinergic synapses. However, the mechanism by which AChE number and density are maintained at the synaptic cleft is poorly understood. In this work, we used fluorescence recovery after photobleaching, photo-unbinding, and quantitative fluorescence imaging to investigate the surface mobility and stability of AChE at the adult innervated neuromuscular junction of living mice. In wild-type synapses, we found that nonsynaptic (perisynaptic and extrasynaptic) AChEs are mobile and gradually recruited into synaptic sites and that most of the trapped AChEs come from the perijunctional pool. Selective labeling of a subset of synaptic AChEs within the synapse by using sequential unbinding and relabeling with different colors of streptavidin followed by time-lapse imaging showed that synaptic AChEs are nearly immobile. At neuromuscular junctions of mice deficient in α-dystrobrevin, a component of the dystrophin glycoprotein complex, we found that the density and distribution of synaptic AChEs are profoundly altered and that the loss rate of AChE significantly increased. These results demonstrate that nonsynaptic AChEs are mobile, whereas synaptic AChEs are more stable, and that α-dystrobrevin is important for controlling the density and stability of AChEs at neuromuscular synapses.

INTRODUCTION

At cholinergic synapses, acetylcholinesterase (AChE) plays a crucial role in synaptic transmission by controlling the action of acetylcholine (Katz and Miledi, 1973; Soreq and Seidman, 2001). The efficacy by which AChE hydrolyzes acetylcholine depends not only on its location but also on the number and density of AChE at synaptic sites. Indeed, reduction in the number and density of AChE leads to failures of neuromuscular transmission. For example, patients with myasthenia syndrome or mice lacking the collagen tailed protein ColQ, perlecan, or dystroglycan (Ohno *et al*., 1998; Feng *et al*., 1999; Jacobson *et al*., 2001; Arikawa-Hirasawa *et al*., 2002) fail to concentrate AChEs at the neuromuscular junction (NMJ), greatly altering synaptic transmission.

At adult sternomastoid NMJs, the density of AChE is estimated to be >3000 molecules/μm^2, composed predominantly of the asymmetric A12 form (Salpeter *et al*., 1972, 1979; Massoulie *et al*., 1993; Anglister *et al*., 1994, 1998). In developing synapses, AChEs are diffusely distributed all along the muscle fiber (Sketelj and Brzin, 1980; Koenig and Rieger, 1981; Fernandez and Seiter, 1984), and they become aggregated at nerve contact sites as synapses mature. Until now, however, it has not been possible to study the mobility of AChE at functioning adult synapses in vivo; therefore, it is not known whether there is a continuous exchange of AChE between nonsynaptic and synaptic zones.

Although the role of the dystrophin glycoprotein complex (DGC) in the maintenance of the postsynaptic receptor density at the neuromuscular junction has been extensively studied (Straub and Campbell, 1997; Grady *et al*., 2000; Akaaboune *et al*., 2002; Burton and Davies, 2002), little is known about the role of this complex on AChE dynamics in the synaptic cleft. In this work, we focused on α-dystrobrevin, a DGC component that has been shown to play a critical role in the maturation and the maintenance of AChR density and turnover at synapses (Grady *et al*., 2000; Akaaboune *et al*., 2002). Because the ratio of AChE to AChR seems to be critical for normal functioning synapses, we sought to investigate the behavior of AChE in synapses deficient in α-dystrobrevin.

Using in vivo fluorescence imaging assays and fasciculin2 snake toxin, which binds selectively to AChE (Martinez-Pena y Valenzuela *et al*., 2005; Krejci *et al*., 2006), we investigated AChE dynamics at individual synapses over time. In the first part of this work, we examined the mobility of synaptic and nonsynaptic AChEs, and we found that nonsynaptic AChEs are free to move on the surface of the muscle fiber and to contribute to synaptic density, whereas synaptic AChEs are immobile. In the second part of this work, we studied AChE dynamics at synapses lacking α-dystrobrevin, and we found that the density and turnover of AChEs are dramatically affected.

MATERIALS AND METHODS

Animals

Non-Swiss albino (NSA) mice (10-wk-old females; 25–30 g) were purchased from Harlan (Indianapolis, IN). Adult α-dystrobrevin–deficient mice (10 wk old; 129SVJ × C57/BL6 hybrid background; Grady *et al*., 2000) were generously provided by Dr. Joshua Sanes (Harvard University), and they were bred in our animal facility. All animal use followed methods approved by the University of Michigan Committee on the Use and Care of Animals.

This article was published online ahead of print in *MBC in Press* (http://www.molbiolcell.org/cgi/doi/10.1091/mbc.E07–02–0093) on May 30, 2007.

Address correspondence to: Mohammed Akaaboune (makaabou@umich.edu).

Toxins

Unlabeled fasciculin2 was purchased from Latoxan (Valence, France), and it was conjugated to biotin using the Biotin-XX Microscale Protein Labeling kit (Invitrogen, Carlsbad, CA). Conjugated bungarotoxin was purchased from Invitrogen. For in vivo imaging of the neuromuscular junction, the mice were anesthetized with an intraperitoneal (i.p.) injection of a mixture of ketamine and xylazine (KX) (17.38 mg/ml). Sternomastoid muscle exposure and neuromuscular junction imaging were done as described in detail previously (Lichtman *et al*., 1987; van Mier and Lichtman, 1994; Akaaboune *et al*., 1999). Briefly, the anesthetized mouse was placed on its back on the stage of a customized fluorescence microscope, and neuromuscular junctions were viewed under a coverslip with a water immersion objective (20× UAPO 0.7 numerical aperture Olympus BW51; Optical Analysis, Nashua, NH) and digital charge-coupled device camera (Retiga EXi, Burnaby, British Columbia, Canada).

Quantitative Fluorescence Imaging

The fluorescence intensity of labeled AChEs at neuromuscular junctions was assayed using a quantitative fluorescence imaging technique, as described by Turney *et al*. (1996), with minor modification. This technique incorporates compensation for image variation that may be caused by spatial and temporal changes in the light source and camera between imaging sessions by calibrating the images at each imaging session with a nonfading reference standard. Image analysis was performed using either a procedure written for IPLab (Scanalytics, Fairfax, VA) or MatLab (Mathworks, Natick, MA). Background fluorescence was approximated by selecting a boundary region around the junction and subtracting it from the original image. The sum of the fluorescent of AChEs at a later time was expressed as the percentage of the sum of fluorescence of AChEs at time 0, which was set at 100%. Average intensity is presented as mean ± SD.

Fluorescence Recovery after Photobleaching Experiments

To investigate the contribution of nonsynaptic (perisynaptic and extrasynaptic) AChEs to the synapse, an argon laser attached to the microscope was used to selectively remove the fluorescence from all synaptically localized AChEs by carefully tracking the branches of the whole neuromuscular junction. The laser illumination was done in the presence of a high concentration of unlabeled streptavidin to prevent the rebinding of unbound fluorescent streptavidin due to photo-unbinding (Akaaboune *et al*., 2002; Akaaboune, Turney, and Lichtman unpublished data). In this way, only nonsynaptic, which include extrasynaptic and perisynaptic, AChEs remained labeled. Acquisition of a second image was used to confirm the removal of fluorescence. From 1–5 d later, the same synapses were reimaged one or multiple times, and the recovery of fluorescence into the bleached area was measured. To study the mobility of AChE, we used fasciculin2-biotin labeling followed by incubation with fluorescent streptavidin conjugate. Fasciculin2-biotin/streptavidin is ideal for this work, because its dissociation from AChE is negligible, and the removal rate of AChE labeled with either fasciculin2-biotin/streptavidin-Alexa or fasciculin2-Alexa is nearly the same. Finally, and most importantly, fasciculin2-biotin/streptavidin is not displaced by unlabeled fasciculin2 (Krejci *et al*., 2006).

To study the contribution of only extrasynaptic AChEs that migrate to the synaptic pool, a laser beam was used to bleach fluorescent conjugates bound to AChEs from synapses and their immediate vicinity ~100 μm away from the synapse along the length of the muscle (Salpeter *et al*., 1988), and a second image was used to confirm the removal of fluorescence. The wound was sutured and the animal was returned to its cage. The same NMJs were then relocated and imaged at subsequent views 2 and 3 d later.

To quantitate the insertion of newly synthesized AChEs, the sternomastoid muscle was saturated with fasciculin2-biotin/streptavidin Alexa 488, and superficial synapses were imaged. An argon laser was used to remove the fluorescence from the synaptic zone, and a second image was taken to confirm the absence of fluorescence. Three days later, the animal was anesthetized, and the same junctions were reimaged and a second dose of fasciculin2-biotin/streptavidin 488 was added to label AChEs that were inserted during this period of time, and images of the same synapses were taken again.

α-Dystrobrevin Mutant Mice

Measurement of AChE Density. To estimate the density of AChEs, the sternomastoid muscle of both adbn$^{-/-}$ mutant and wild-type mice were saturated with either fasciculin2-Alexa 594 (7 μg/ml; 3 h), or fasciculin2-biotin (7 μg/ml; 3 h) followed by a saturating dose of streptavidin-Alexa 488/594 (10 μg/ml; 3 h). The superficial neuromuscular junctions were imaged, and the mean fluorescence was determined using a quantitative fluorescence assay.

Loss and Insertion Rates of Fluorescent Labeled AChEs. To determine the loss rate of AChE from wild-type and adbn$^{-/-}$ mutant synapses, the sternomastoid muscle was labeled with a low dose of fasciculin2-biotin (5 μg/ml; 30 min) (usually <40% of AChEs are labeled) followed by a saturating dose of streptavidin-Alexa 488. Usually, the first views of superficial synapses were taken after 1 d of initial labeling, to allow the clearance of unbound fasciculin2-biotin. On subsequent days, the same synapses were located and reimaged one or multiple times, and their fluorescence intensities were assayed. To determine the insertion rate of AChE in α-dystrobrevin mutant mice, the sternomastoid muscle was saturated with fasciculin2-biotin/streptavidin-Alexa 488 and imaged. Twenty-four hours later, the synapses were imaged, saturated with fresh fasciculin2-biotin/streptavidin-Alexa 488, and reimaged.

Photo-Unbinding. We used this technique to follow exclusively the movement of synaptic AChEs within single synapses from the same muscle fiber. This method allows the labeling of different populations of AChEs at the same NMJ with distinct fluorophores. The sternomastoid muscle was labeled with a low dose of fasciculin2-biotin (so synaptic activity remains functional) followed by a saturating dose of streptavidin-Alexa 488. Photo-unbinding was then performed as described by Akaaboune *et al*. (2002). Briefly, an argon laser (488 nm), 1–2 mW at the back aperture of the objective, was used to excite fluorescently labeled fasciculin2-biotin/streptavidin-Alexa 488 until all fluorescence was removed. Immediately, the sternomastoid muscle was incubated in the presence of saturating dose of a different color of streptavidin conjugated to Alexa 594 to selectively label the laser-illuminated region. The doubly labeled junctions were imaged, and the wound was then sutured. The same synapses were reimaged again 1–2 d later.

Confocal Imaging. To determine the distribution of AChE at the synaptic cleft, the sternomastoid muscles of both wild-type and mutant synapses were labeled with fluorescent α-bungarotoxin-Alexa 594 and fasciculin2-Alexa 488, and then they were perfused with 4% paraformaldehyde. The sternomastoid muscles were dissected and mounted on slides, and then they were scanned using confocal microscopy (Olympus FV500; Olympus America, Melville, NY).

RESULTS

Migration of Nonsynaptic AChEs to Synaptic Areas

As a first step, we asked whether labeled AChEs that are initially nonsynaptic (perisynaptic and extrasynaptic) can migrate into synaptic sites in living muscle. To do this, the sternomastoid muscle of mice was bathed with a subsaturating dose of fasciculin2-biotin followed by a single dose of streptavidin-Alexa 488 to saturate all biotin sites. After the initial labeling (usually 1 d, to allow time for clearance of any unbound toxin), superficial neuromuscular junctions were imaged, and an argon laser was used to selectively remove the fluorescence from all synaptically localized AChEs by tracking the branches of the whole neuromuscular junction. In this way, only the nonsynaptic AChEs remained fluorescently labeled. Confirmation of the removal of fluorescence was done by acquiring an image (Figure 1A). Photobleaching was performed in the presence of unlabeled streptavidin to prevent the rebinding of streptavidin-Alexa 488 to biotin fasciculin2 after photo-unbinding (Akaaboune *et al*., 2002; Akaaboune, Turney, Sanes, and Lichtman, unpublished data). We then monitored the recovery of fluorescence at bleached junctions over time. We found that over the next 24 h, junctions gained 2.4 ± 0.7% (mean ± SD; n = 32) of their original fluorescence (Figure 1C). The intensity of fluorescence recovery gradually increased to reach 4 ± 1% (n = 19) and 5 ± 1.2% (n = 27) at 48 and 72 h, respectively (Figure 1). At 5 d, the fluorescence recovery at bleached synapses, however, declined to 2.2 ± 1% (n = 10). When synapses were labeled and not photobleached, they lost 17 ± 8% (n = 51) of their fluorescence intensity per day (Figure 4). Thus, the fluorescence recovery observed after photobleaching suggests that a significant number of nonsynaptic AChEs migrate into the synaptic zone (see *Discussion*). To rule out the possibility of that the recovery of fluorescence observed in living muscle was due to reversible bleaching of the fluorophore or to the rebinding of labeled toxin, a sternomastoid muscle was first fixed with 2% paraformaldehyde, labeled with fasciculin2-biotin/streptavidin-Alexa 488, illuminated with laser to remove fluorescence, and then transplanted into the neck of a host mouse directly next to

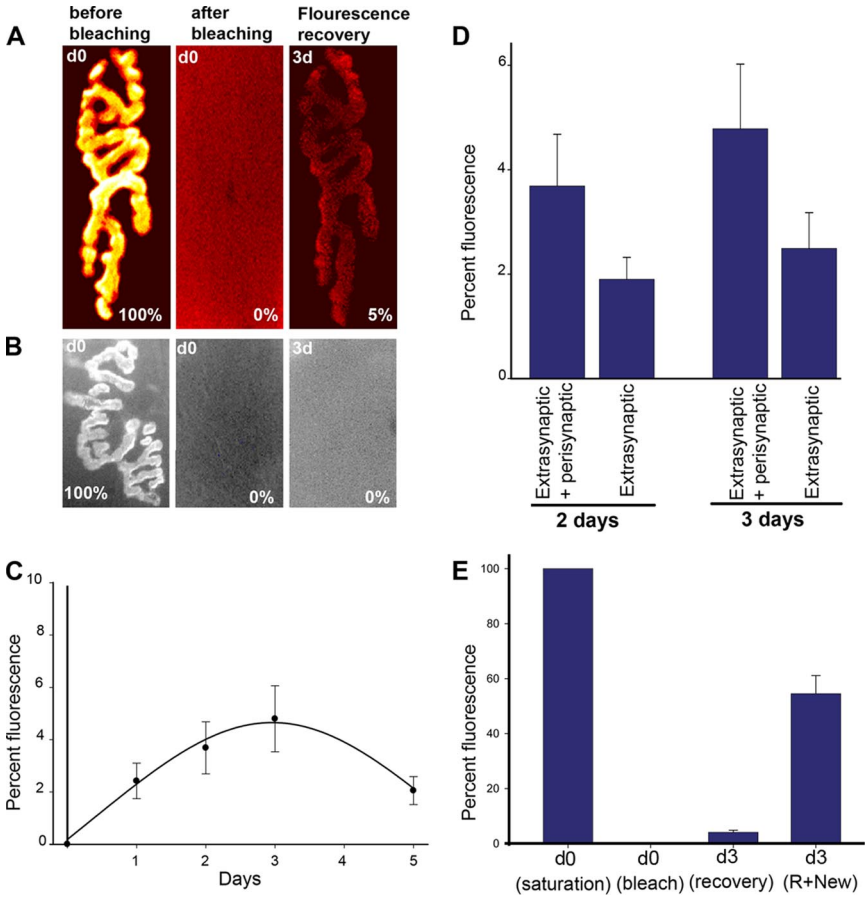

Figure 1. Time-lapse imaging of AChE mobility on a muscle fiber in vivo. (A) Example of a neuromuscular junction that was imaged three times over 3 d, showing that nonsynaptic AChEs migrate into the junctional bleached synapse. After removing all the fluorescence from the junction by tracking the branches with a focused laser, a second image was acquired to confirm the removal of fluorescence. The fluorescence recovery due to migration was 5% at 3 d (despite AChE turnover). However, in sternomastoid muscle that was fixed, labeled, and transplanted in the neck of a host mouse, there was no evidence of recovery of fluorescence intensity over the same time period (B). This indicates that the recovery of fluorescence intensity is not due to reversible bleaching of the fluorophore. (C) Graph summarizes fluorescence recovery in many junctions followed over time. (D) The sternomastoid muscle was labeled with fasciculin2-biotin/streptavidin-Alexa 488, and the perisynaptic and synaptic AChEs were bleached (along the length of up to the muscle ~100 μm away from the synapse zone). Histogram shows the fluorescence recovery when synaptic and perisynaptic regions were bleached, and when only synaptic regions were bleached. (E) Histogram shows that most of the AChEs are inserted directly in the synaptic cleft. Each data point represents the mean percentage of the original fluorescence intensity ± SD.

the living sternomastoid muscle. No recovery of original fluorescence into bleached synapses was observed over time (Figure 1B).

We next asked whether immediate perisynaptic or distal extrasynaptic regions served as the major source of nonsynaptic AChEs that migrate to the synaptic pool. To do this, we compared the amount of recovery between junctions in which all of the nonsynaptic AChEs were labeled and junctions in which the majority of the perisynaptic AChEs were bleached. When all the fluorescence of synaptic and perisynaptic AChEs was removed, only 2 ± 0.4% (n = 7) and 2.5 ± 0.7% (n = 11) of the original junctional fluorescence recovered after 48 and 72 h, respectively (compared with ~4 and 5% when only fluorescently tagged junctional AChEs were bleached) (Figure 1D). This result implies that a significant amount of fluorescence recovery is due to the migration of AChEs that are located within 100 μm of the synaptic area. and it suggests that perisynaptic AChEs play a role in maintaining synaptic AChE density. We next wanted to determine the amount of AChEs that have been inserted directly into synaptic sites. To do this, the sternomastoid muscle was bathed with a saturating dose of fasciculin2-biotin/streptavidin-Alexa 488 to label both nonsynaptic and synaptic AChEs. The superficial synapses were then imaged, laser illuminated, and reimaged to confirm complete photobleaching of the synapses. Three days later, the same synapses were relocated and reimaged, and then saturating doses of fasciculin2-biotin and streptavidin-Alexa 488 were added to label newly inserted AChEs. We found that the fluorescence in synapses increased significantly to reach 55 ± 7% (n = 6) of original fluorescence (Figure 1E). These results support the idea that the majority of AChEs are inserted directly into synaptic sites.

Synaptic AChEs Are Immobile within the Neuromuscular Junction

Having found that nonsynaptic AChEs can move into synaptic sites, we next asked whether synaptic AChEs can migrate from one region to another within the same synapse. To assay the mobility of synaptic AChEs without contamination from nonsynaptic AChEs, the sternomastoid muscle was incubated with fasciculin2-biotin (labeling both synaptic and nonsynaptic AChEs), and biotin sites were saturated with streptavidin-Alexa 488. An argon laser was then used to selectively unbind green streptavidin-labeled AChEs from a small region within a junction, which was then relabeled with streptavidin Alexa 594 (red), as described previously (Akaaboune *et al.*, 2002). When mobility of the red-labeled synaptic AChEs was monitored after 1 or 2 d after the initial labeling, we found that the red-labeled AChEs did not spread from their initial region into the rest of the junction, despite the overall loss of red fluorescence. Green fluorescence, however, was seen in the bleached region (Figure 2). This indicates that synaptic AChEs are almost entirely immobile within the synaptic zone, at least during the window of our experiments (see *Discussion*). and it implies that the removal of synaptic AChEs occurs locally.

AChE Dynamics at Synapses Lacking α-Dystrobrevin

Previous studies have shown that the loss of α-dystrobrevin dramatically affects the density and the number of postsynaptic AChRs (Grady *et al.*, 2000, 2003; Akaaboune *et al.*,

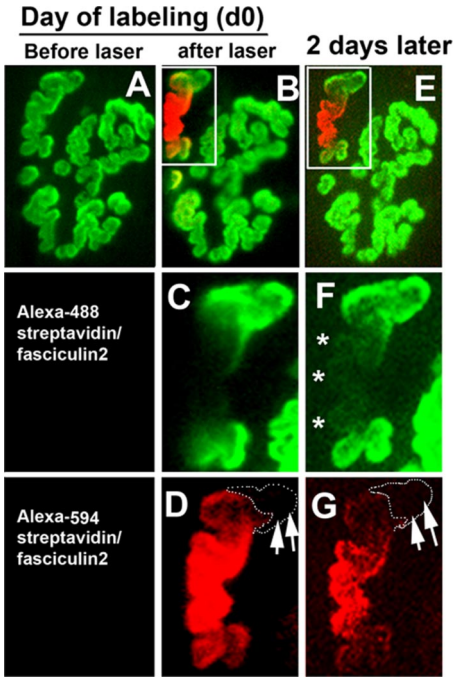

Figure 2. Time-lapse imaging to determine synaptic AChE mobility in vivo. (A) Junctions were labeled with fasciculin2-biotin followed with a single saturating dose of (green) streptavidin-Alexa 488. (B) A laser was used to unbind green streptavidin within a small region of the junction, and then a second dose of (red) streptavidin-Alexa 594 was added to label AChE that had lost their green streptavidin. (C and D) High-power view of the area that was photo-unbound and relabeled in B (box). When the same synapse was imaged 2 d later (E), there was no evidence for the mixing of red and green fluorescence, as indicated by arrows and dashed lines. (F and G) High-power view of the area indicated in box (E). In the bleached area, there was some recovery of green fluorescence, which most likely is due the migration of nonsynaptic AChEs (asterisks). This indicates that synaptic AChE labeled with red fluorescence is immobile, whereas nonsynaptic AChE is mobile.

2002). Because the ratio of AChE to AChR is critical for normal synaptic functioning, we wanted to examine whether AChE density and turnover rate are also affected by the loss of α-dystrobrevin. First, we wanted to determine the relative distribution of AChEs to AChRs in mutant mice lacking α-dystrobrevin (adbn$^{-/-}$). To do this, AChRs and AChEs at the sternomastoid muscle were both labeled with distinctive fluorophore-tagged toxins (α-bungarotoxin-Alexa 594 for AChRs and fasciculin2-Alexa 488 for AChEs). Mice were then perfused with 4% paraformaldehyde, and sternomastoid muscles were dissected and mounted on slides and then scanned using confocal microscopy. In wild-type synapses, AChE staining extended beyond the AChR staining (Figure 3A), as reported previously (Adams *et al*., 2000; Krejci *et al*., 2006). However, in adbn$^{-/-}$ synapses, AChE staining was disorganized and resembled AChR distribution, which displays a granular appearance with frequent speckles of AChRs. AChE staining was absent from these speckles, probably because the folds are absent in such areas (Grady *et al*., 2000). This observation indicates that despite the intracellular localization of adbn, it is involved in the clustering and organization not only of AChRs but also of AChEs at the synapse (Figure 3, A–F).

Next, we wanted to determine whether the number and the density of AChEs are affected in synapses of adbn$^{-/-}$ mice. To do so, the sternomastoid muscles of both mutant and wild-type mice were labeled with fluorescent fasciculin2 (7 μg/ml; 3 h) to saturate all AChEs, and the superficial NMJs were imaged using a quantitative fluorescence assay. We found that the density of AChE in adbn$^{-/-}$ NMJs was decreased to ~30% of those in normal junctions, whereas the overall size of synapses in mutant mice remained similar to that of wild type (Figure 3). This result suggests that α-dystrobrevin plays an important role in maintaining the density of AChE at the synapse. AChRs are also reduced by similar amounts in muscles of the adbn$^{-/-}$ mice (Akaaboune *et al*., 2002), suggesting that AChE and AChR are present in an equal ratio at wild-type and adbn$^{-/-}$ synapses.

We asked whether the low density of AChE observed in adbn$^{-/-}$ synapses is associated with a rapid removal of AChE from the synapse or with a failure to properly insert AChE into the basal lamina. The rate of AChE removal from adbn$^{-/-}$ synapses was examined by labeling the sternomastoid muscle of mutant and wild-type mice with fasciculin2-biotin/streptavidin-Alexa 488 and by imaging superficial synapses. The fluorescence intensity of superficial neuromuscular junctions was measured at time 0, and then 1, 2, and 3 d later. We found that after initial labeling, AChE fluorescence intensity was decreased by 35 ± 10% (n = 59) at 1 d and by 49 ± 10% (n = 52) and 55 ± 9% (n = 27) at 2 and 3 d, respectively. At wild-type synapses, however, the loss was only 17 ± 8 (n = 51) at 1 d, 29 ± 8% (n = 54) at 2 d, and 34 ± 9% (n = 43) at 3 d (Figure 4, A–C). This rapid loss rate suggests that adbn is involved in controlling the lifetime of AChEs in the synaptic cleft. We next asked whether the low density of AChEs observed in mutant synapses is a consequence of a decreased insertion of newly synthesized AChEs, knowing that the shape of the synapses of these mutants remains constant at least over the time course of the experiments. To do this, the sternomastoid muscle of adbn$^{-/-}$ mice was saturated with fasciculin2-biotin followed with a saturating dose of streptavidin-Alexa 488, and then superficial synapses were imaged. When synapses were reimaged on subsequent days, we found that AChE insertion (determined when new fasciculin2-biotin/streptavidin-Alexa 488 was added) nearly matched AChE loss (Figure 4D). These results argue that despite the accelerated rate of AChE loss, the total number of AChEs was maintained by AChE insertion. To determine whether the increased rate of AChE loss in adbn$^{-/-}$ is due to a disassembly of anchoring molecules dystroglycan and/or perlecan, we performed immunostaining on the sternomastoid muscle with antibodies to dystroglycan and perlecan. We found that the distribution of these anchoring proteins in *adbn*$^{-/-}$ muscle are not altered (data not shown), as has been shown previously (Grady *et al*., 1999).

It seemed possible that the mobility of AChE would also be affected by the loss of α-dystrobrevin from the postsynaptic membrane in mutant synapses. To investigate this, the sternomastoid muscle was labeled with a low dose of fasciculin2-biotin followed by a single saturating dose of streptavidin-Alexa 488 (as described above), and then superficial synapses were imaged. The synapses were laser illuminated to remove fluorescence from the NMJ, and they were immediately imaged to confirm complete bleaching. At 3 d, when maximum recovery was observed at wild-type synapses, adbn$^{-/-}$ synapses showed very little fluorescence recovery (2.4 ± 0.5%; n = 20); and in many cases. the fluorescence intensity was so low that it was very difficult to accurately quantify (Figure 4E).

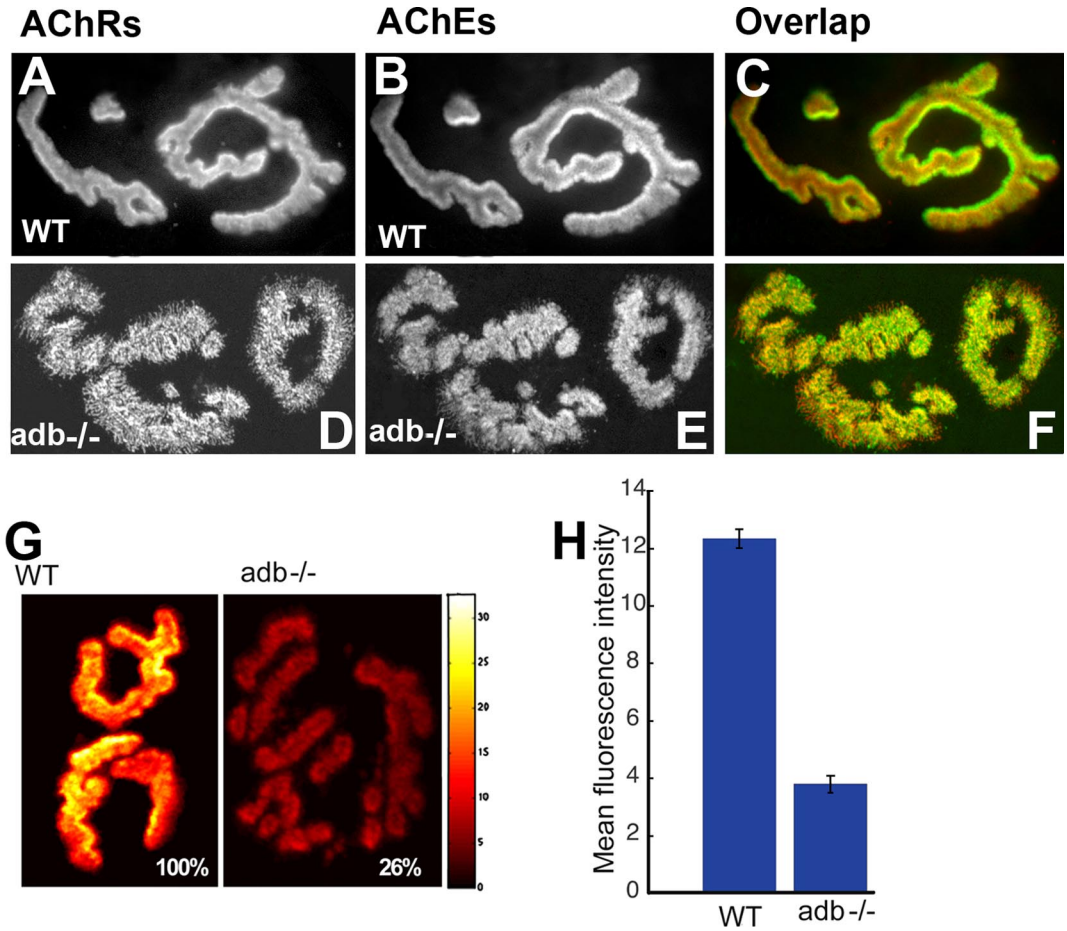

Figure 3. Confocal images of wild-type and α-dystrobrevin$^{-/-}$ neuromuscular junctions. (A and B) Example of an adult wild-type mouse neuromuscular junction doubly labeled with fasciculin2-Alexa 488 (AChEs, green) and α-bungarotoxin-Alexa 594 (AChRs, red). (D and E) Distribution of AChRs and AChEs at the neuromuscular junction of α-dystrobrevin$^{-/-}$ mutant mouse. (C and F) Overlap of green and red. Note that receptors staining exhibit a granular appearance in the adbn$^{-/-}$ mice with speckles extending beyond the junctional branches (Grady *et al*., 2003); AChEs staining shows a similar pattern, except for the absence of AChE in speckles. In contrast, wild-type mouse NMJ shows clear striations of both AChRs and AChEs. (G) Example of a superficial junction in which AChEs are labeled with fasciculin2-Alexa 594 and imaged using a quantitative fluorescence imaging assay. Pseudocolor images provided a linear representation of the density of AChEs. (H) The graph summarizes the data obtained from multiple neuromuscular junctions. Note that the density of AChEs is severely reduced in adbn$^{-/-}$ mutant NMJs compared with wild type. Each data point represents the mean percentage of fluorescence intensity ± SD.

DISCUSSION

This work provides the first evidence that AChE is mobile in the nonsynaptic compartment and can shuttle from nonsynaptic to synaptic zones, whereas synaptic AChE is immobile on the living muscle. In addition, this work demonstrates that α-dystrobrevin, a component of the dystrophin glycoprotein complex, controls the density, distribution, and the lifetime of extracellular AChEs at synaptic sites.

Although it is not clear how diffusion of AChE in the nonsynaptic regions occurs, this work unambiguously shows that AChE can move from nonsynaptic to synaptic areas on the living muscle fiber. Given the high density of AChE in the synaptic cleft (~3000 AChEs/μm^2) (Salpeter *et al*., 1978; Anglister *et al*., 1994, 1998) and its high rate of removal from synapses (17%/d), the nonsynaptic AChEs may contribute to maintaining the high density of synaptic AChE despite the fact that the majority of AChEs are directly inserted into synaptic sites. Because AChE has been shown to not recycle back to the synaptic cleft (Bruneau *et al*., 2005), it is likely that insertion of AChE followed by diffusion and trapping of AChE in the NMJ is the main mechanism by which nonsynaptic AChE contributes to AChE synaptic density. Consistent with this, it has been shown that either endogenously deposited or experimentally transplanted AChE can be recruited and aggregated at the postsynaptic membrane (Rotundo *et al*., 1997). In developing muscle fibers, AChEs are found to be distributed diffusely over the muscle fiber, and they aggregate progressively into the synaptic zone as synapses mature (Sketelj and Brzin, 1980; Koenig and Rieger, 1981; Fernandez and Seiter, 1984; Legay *et al*., 1995). A similar developmental pattern has been described for AChRs (Anderson and Cohen, 1977; Ziskind-Conhaim *et al*., 1984). Lateral movement of AChE was also previously reported in cultured muscle cells (Peng *et al*., 1999). That both AChEs and AChRs are distributed diffusely along the muscle fiber surface, subsequently become aggregated at nerve muscle contacts, and migrate from nonsynaptic to synaptic zones may suggest that they share similar regulatory mechanisms. A constant ratio of AChE to AChR may be critical to ensure a normal, stable and effective physiological response at neuromuscular synapses.

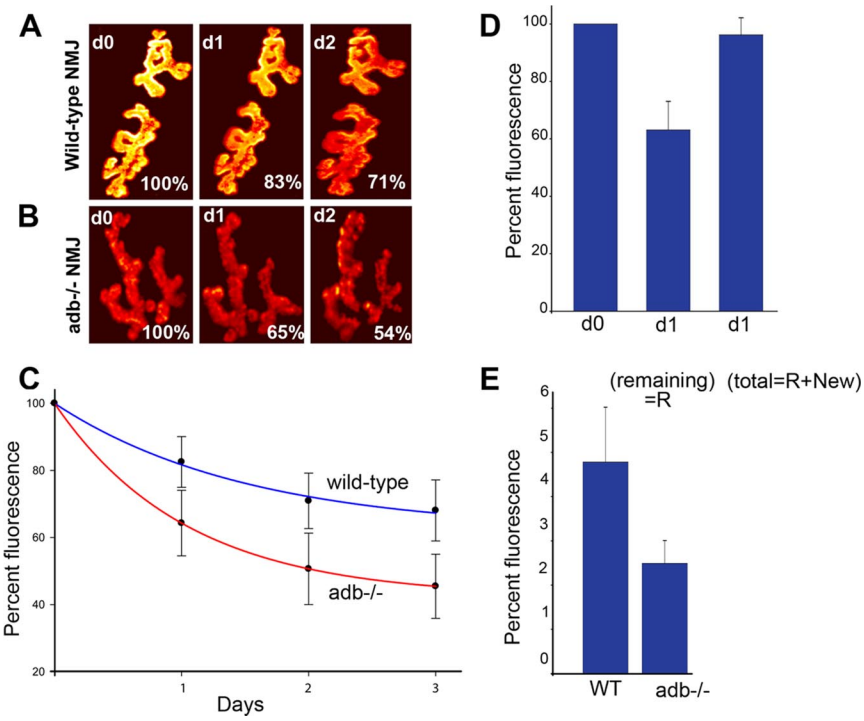

Figure 4. AChE lifetime is dramatically affected in α-dystrobrevin$^{-/-}$ neuromuscular Junctions. (A and B) Example of neuromuscular junctions of wild-type and α-dystrobrevin$^{-/-}$ mice imaged over 2 d. The loss rate of AChEs is significantly increased in the adbn$^{-/-}$ compared with wild-type synapses (B). The total fluorescence intensity of fasciculin2-biotin/streptavidin-Alexa 488 was expressed as 100% at the first view of images. (C) The graph shows the loss of fluorescence over 3 d after a low, subsaturating dose of fasciculin2-biotin/streptavidin-Alexa 488 (so synaptic activity was not completely disrupted). These results indicate that α-dystrobrevin somehow controls the stability of AChEs in the synaptic cleft. (D) Histogram shows results of AChE loss and insertion after 24 h. Note that nearly all lost AChEs were replaced by new AChEs inserted into the NMJ. This result indicates that in adbn$^{-/-}$, the insertion of newly synthesized AChEs is not affected. (E) Histogram shows the mobility of AChEs at the adbn$^{-/-}$ NMJs after 3 d. Note that few AChEs were recovered at the synaptic bleached area, suggesting that that the low recovery may be the result of high turnover of AChE in these mutant synapses. Each data point represents the mean percentage of original fluorescence intensity ± SD.

One question our data raises is how AChE movement on the muscle surface may occur. Extensive studies have shown that AChE is anchored in the extracellular matrix through the collagen protein ColQ (Krejci *et al*., 1997), which in turn forms complexes with different acceptor molecules (Rotundo, 2003; Rotundo *et al*., 2005). Thus, it is possible that the diffusion trap mechanism observed on living muscle could be the result of the migration of AChE–ColQ complexes. If this is the case, it would suggest that the ColQ–AChE complex is highly dynamic despite its large size and multiple interactions with other proteins, and it is possible that other components of the extracellular matrix are also dynamic throughout the lifetime of a synapse. Biochemical analyses of the sedimentation patterns of muscle extracts have shown that AChE forms are expressed differentially in fast and slow twitch muscles. For example, in the mature sternomastoid muscle (fast muscle), A_{12} is the predominant form of AChE found at end plates, whereas A_4 and A_8 forms are present in the nonsynaptic zone of the soleus (slow muscle) (Krejci *et al*., 1999). It is conceivable that the sternomastoid muscle also produces a small quantity of A_8 and A_4 isoforms in its nonsynaptic segments while directly inserting A_{12} into the endplate. Alternatively, it is possible that the recovery seen in bleached synapses may correspond to the Proline Rich Membrane Anchor protein (PRiMA)/AChE population. Indeed, it has been shown that PRiMA can organize AChE tetramers and anchor them in plasma membranes (Perrier *et al*., 2002), although the proportion of AChE anchored by PRiMA in the plasma membrane remains unsolved. In any event, it would be interesting to study the mobility of AChE in mice deficient in PRiMA.

In contrast to nonsynaptic AChE mobility, our data argue that synaptic AChE is almost entirely immobile or that it has a very slow diffusion within the synapse, at least in the time period of our analyses. Whether manipulation of synaptic activity would alter the mobility of this AChE population remains to be seen. AChE gene expression has been shown to be sensitive to electrical activity (Michel *et al*., 1994). Our data indicate that the majority of AChE at synapses is directly inserted into synaptic cleft (Figure 1E). These results are supported by previous reports showing the presence of high local expression of both AChE and ColQ mRNAs in fast muscles (Jasmin *et al*., 1993; Legay *et al*., 1995; Krejci *et al*., 1999). However, the lack of the mobility of synaptic AChE may indicate that this population of AChE is tethered very tightly in synaptic basal lamina through the scaffold ColQ-perlecan-dystroglycan. Interestingly, in mice deficient in perlecan and dystroglycan, AChE is undetectable (Jacobson *et al*., 2001; Arikawa-Hirasawa *et al*., 2002); and more recently, it has been shown that AChE anchoring in heterologous cell systems requires muscle-specific kinase through its interaction with the C terminus of ColQ (Cartaud *et al*., 2004).

At present, it is not clear how intracellular alpha dystrobrevin protein could affect extracellular matrix AChE stability, because it does not link directly to AChEs. A reduction or absence of AChE clusters has been reported in the synapses of several mouse mutants. For example in mice deficient in perlecan, AChE is totally lacking at neuromuscular synapses (Arikawa-Hirasawa *et al*., 2002), and AChE is significantly reduced or no longer concentrated at dystroglycan null synapses (Jacobson *et al*., 2001). Similarly, in mice deficient in the protein rapsyn, which is associated with AChRs, AChRs do not cluster and AChE aggregates also fail to form at synaptic sites, suggesting that rapsyn–AChR interaction is also essential for aggregation of AChE at the basal lamina. In the present work, we report that the density and turnover rate of AChEs are dramatically affected in adbn$^{-/-}$ synapses (Figures 3 and 4). Because most removed AChEs were replaced by newly synthesized ones, our findings suggest that adbn may be involved in AChE stability rather than synthesis. As with AChE, we previously showed that the density and turnover rate of AChRs are also significantly affected in adbn$^{-/-}$ synapses (Grady *et al*., 2000; Akaaboune *et al*., 2002). These findings, along with our previous results on AChR dynamics, clearly show that there is a correlation

between number and lifetime of AChEs and the number and lifetime of AChRs at individual synapses. Although it is not clear that a direct interaction exists between AChR and AChE, it is possible that the loss of α-dystrobrevin primarily affects the number of AChRs through changes in conformation of the DGC and/or its association with other postsynaptic components; changes in AChRs in turn may affect the number and stability of AChE. This idea is supported by the following evidence: 1) there are no AChE clusters when AChR clusters do not form (De La Porte *et al*., 1998); 2) when the number of AChRs decreases, the number of AChEs decreases by the same magnitude; and 3) when the turnover of AChR increases the AChE turnover rate also increases. Clustering of AChR could be the starting point for accumulation of AChE, although there is no evidence to date for a direct interaction between AChR and AChE. Nevertheless, it has been shown that the loss of AChE can control the density of AChRs. For example, in mutants lacking ColQ (in which AChE fails to concentrate at the synapse) or in $AChE^{-/-}$ mutants, receptor density is significantly decreased (Feng *et al*., 1999; Xie *et al*., 2000). It would be interesting to determine whether AChE lifetime is affected in these mice. An alternative idea to account for adbn effects on AChE is that the high turnover rate and low number of AChE results from a reduction of dystroglycan, which provides a molecular link between the basal lamina and intracellular scaffold proteins. However, previous studies and our data argue against this possibility, because neither perlecan nor dystroglycan seem to be affected by the loss of $adbn^{-/-}$ (Grady *et al*., 1999). It is possible that the loss of α-dystrobrevin may indirectly reduce the level of other DGC components that, in turn, interact with other extracellular synaptic components, thereby altering the stability of AChE. For example, a similar phenotype was observed in mutant mice lacking α-syntrophin, another component of the DGC, in which AChRs and AChEs are decreased at the NMJ (Adams *et al*., 2000).

ACKNOWLEDGMENTS

We thank the members of our laboratory and Drs. John Kuwada, Richard Hume, Krejci Eric, and Amy Chang for helpful discussions about this work and Dr. Joshua Sanes for providing a pair of α-dystrobrevin mutant mice. This work was supported by the University of Michigan, National Institute of Neurological Disorders and Stroke Research grant NS-047332 (to M.A.).

REFERENCES

Adams, M. E., Kramarcy, N., Krall, S. P., Rossi, S. G., Rotundo, R. L., Sealock, R., and Froehner, S. C. (2000). Absence of alpha-syntrophin leads to structurally aberrant neuromuscular synapses deficient in utrophin. J. Cell Biol. *150*, 1385–1398.

Akaaboune, M., Culican, S. M., Turney, S. G., and Lichtman, J. W. (1999). Rapid and reversible effects of activity on acetylcholine receptor density at the neuromuscular junction in vivo. Science *286*, 503–507.

Akaaboune, M., Grady, R. M., Turney, S., Sanes, J. R., and Lichtman, J. W. (2002). Neurotransmitter receptor dynamics studied in vivo by reversible photo-unbinding of fluorescent ligands. Neuron *34*, 865–876.

Anderson, M. J., and Cohen, M. W. (1977). Nerve-induced and spontaneous redistribution of acetylcholine receptors on cultured muscle cells. J. Physiol. *268*, 757–773.

Anglister, L., Eichler, J., Szabo, M., Haesaert, B., and Salpeter, M. M. (1998). 125I-Labeled fasciculin 2, a new tool for quantitation of acetylcholinesterase densities at synaptic sites by EM-autoradiography. J. Neurosci. Methods *81*, 63–71.

Anglister, L., Stiles, J. R., and Salpeter, M. M. (1994). Acetylcholinesterase density and turnover number at frog neuromuscular junctions, with modeling of their role in synaptic function. Neuron *12*, 783–794.

Arikawa-Hirasawa, E., Rossi, S. G., Rotundo, R. L., and Yamada, Y. (2002). Absence of acetylcholinesterase at the neuromuscular junctions of perlecan-null mice. Nat. Neurosci *5*, 119–123.

Bruneau, E., Sutter, D., Hume, R. I., and Akaaboune, M. (2005). Identification of nicotinic acetylcholine receptor recycling and its role in maintaining receptor density at the neuromuscular junction in vivo. J. Neurosci. *25*, 9949–9959.

Burton, E. A., and Davies, K. E. (2002). Muscular dystrophy–reason for optimism? Cell *108*, 5–8.

Cartaud, A., Strochlic, L., Guerra, M., Blanchard, B., Lambergeon, M., Krejci, E., Cartaud, J., and Legay, C. (2004). MuSK is required for anchoring acetylcholinesterase at the neuromuscular junction. J. Cell Biol. *165*, 505–515.

De La Porte, S., Chaubourt, E., Fabre, F., Poulas, K., Chapron, J., Eymard, B., Tzartos, S., and Koenig, J. (1998). Accumulation of acetylcholine receptors is a necessary condition for normal accumulation of acetylcholinesterase during in vitro neuromuscular synaptogenesis. Eur. J. Neurosci. *10*, 1631–1643.

Feng, G., Krejci, E., Molgo, J., Cunningham, J. M., Massoulié, J., and Sanes, J. R. (1999). Genetic analysis of collagen Q: roles in acetylcholinesterase and butyrylcholinesterase assembly and in synaptic structure and function. J. Cell Biol. *144*, 1349–1360.

Fernandez, H. L., and Seiter, T. C. (1984). Subcellular distribution of acetylcholinesterase asymmetric forms during postnatal development of mammalian skeletal muscle. FEBS Lett. *170*, 147–151.

Grady, R. M., Akaaboune, M., Cohen, A. L., Maimone, M. M., Lichtman, J. W., and Sanes, J. R. (2003). Tyrosine-phosphorylated and nonphosphorylated isoforms of alpha-dystrobrevin: roles in skeletal muscle and its neuromuscular and myotendinous junctions. J. Cell Biol. *160*, 741–752.

Grady, R. M., Grange, R. W., Lau, K. S., Maimone, M. M., Nichol, M. C., Stull, J. T., and Sanes, J. R. (1999). Role for alpha-dystrobrevin in the pathogenesis of dystrophin-dependent muscular dystrophies. Nat. Cell Biol. *1*, 215–220.

Grady, R. M., Zhou, H., Cunningham, J. M., Henry, M. D., Campbell, K. P., and Sanes, J. R. (2000). Maturation and maintenance of the neuromuscular synapse: genetic evidence for roles of the dystrophin–glycoprotein complex. Neuron *25*, 279–293.

Jacobson, C., Cote, P., Rossi, S., Rotundo, R., and Carbonetto, S. (2001). The dystroglycan complex is necessary for stabilization of acetylcholine receptor clusters at neuromuscular junctions and formation of the synaptic basement membrane. J. Cell Biol. *152*, 435–450.

Jasmin, B. J., Lee, R. K., and Rotundo, R. L. (1993). Compartmentalization of acetylcholinesterase mRNA and enzyme at the vertebrate neuromuscular junction. Neuron *11*, 467–477.

Katz, B., and Miledi, R. (1973). The binding of acetylcholine to receptors and its removal from the synaptic cleft. J. Physiol. *231*, 549–574.

Koenig, J., and Rieger, F. (1981). Biochemical stability of the AChE molecular forms after cytochemical staining: postnatal focalization of the 16S AChE in rat muscle. Dev. Neurosci. *4*, 249–257.

Krejci, E., Legay, C., Thomine, S., Sketelj, J., and Massoulie, J. (1999). Differences in expression of acetylcholinesterase and collagen Q control the distribution and oligomerization of the collagen-tailed forms in fast and slow muscles. J. Neurosci. *19*, 10672–10679.

Krejci, E., Martinez-Pena y Valenzuela, I., Ameziane, R., and Akaaboune, M. (2006). Acetylcholinesterase dynamics at the neuromuscular junction of live animals. J. Biol. Chem. *281*, 10347–10354.

Krejci, E., Thomine, S., Boschetti, N., Legay, C., Sketelj, J., and Massoulié, J. (1997). The mammalian gene of acetylcholinesterase-associated collagen. J. Biol. Chem. *272*, 22840–22847.

Legay, C., Huchet, M., Massoulie, J., and Changeux, J. P. (1995). Developmental regulation of acetylcholinesterase transcripts in the mouse diaphragm: alternative splicing and focalization. Eur. J. Neurosci. *7*, 1803–1809.

Lichtman, J. W., Magrassi, L., and Purves, D. (1987). Visualization of neuromuscular junctions over periods of several months in living mice. J. Neurosci. *7*, 1215–1222.

Martinez-Pena y Valenzuela, I., Hume, R. I., Krejci, E., and Akaaboune, M. (2005). In vivo regulation of acetylcholinesterase insertion at the neuromuscular junction. J. Biol. Chem. *280*, 31801–31808.

Massoulie, J., Pezzementi, L., Bon, S., Krejci, E., and Vallette, F. M. (1993). Molecular and cellular biology of cholinesterases. Prog. Neurobiol. *41*, 31–91.

Michel, R. N., Vu, C. Q., Tetzlaff, W., and Jasmin, B. J. (1994). Neural regulation of acetylcholinesterase mRNAs at mammalian neuromuscular synapses. J. Cell Biol. *127*, 1061–1069.

Ohno, K., Brengman, J., Tsujino, A., and Engel, A. G. (1998). Human endplate acetylcholinesterase deficiency caused by mutations in the collagen-like tail subunit (ColQ) of the asymmetric enzyme. Proc. Natl. Acad. Sci. USA *95*, 9654–9659.

Peng, H. B., Xie, H., Rossi, S. G., and Rotundo, R. L. (1999). Acetylcholinesterase clustering at the neuromuscular junction involves perlecan and dystroglycan. J. Cell Biol. *145*, 911–921.

Perrier, A., Massoulié, J., and Krejci, E. (2002). PRiMA: the membrane anchor of acetylcholinesterase in brain. Neuron *33*, 275–285.

Rotundo, R. L. (2003). Expression and localization of acetylcholinesterase at the neuromuscular junction. J. Neurocytol. *32*, 743–766.

Rotundo, R. L., Rossi, S. G., and Anglister, L. (1997). Transplantation of quail collagen-tailed acetylcholinesterase molecules onto the frog neuromuscular synapse. J. Cell Biol. *136*, 367–374.

Rotundo, R. L., Rossi, S. G., Kimbell, L. M., Ruiz, C., and Marrero, E. (2005). Targeting acetylcholinesterase to the neuromuscular synapse. Chem. Biol. Interact. *157–158*, 15–21.

Salpeter, M. M., Kasprzak, H., Feng, H., and Fertuck, H. (1979). Endplates after esterase inactivation in vivo: correlation between esterase concentration, functional response and fine structure. J. Neurocytol. *8*, 95–115.

Salpeter, M. M., Marchaterre, M., and Harris, R. (1988). Distribution of extrajunctional acetylcholine receptors on a vertebrate muscle: evaluated by using a scanning electron microscope autoradiographic procedure. J. Cell Biol. *106*, 2087–2093.

Salpeter, M. M., Plattner, H., and Rogers, A. W. (1972). Quantitative assay of esterases in end plates of mouse diaphragm by electron microscope autoradiography. J. Histochem. Cytochem. *20*, 1059–1068.

Salpeter, M. M., Rogers, A. W., Kasprzak, H., and McHenry, F. A. (1978). Acetylcholinesterase in the fast extraocular muscle of the mouse by light and electron microscope autoradiography. J. Cell Biol. *78*, 274–285.

Sketelj, J., and Brzin, M. (1980). 16 S acetylcholinesterase in endplate-free regions of developing rat diaphragm. Neurochem. Res. *5*, 653–658.

Soreq, H., and Seidman, S. (2001). Acetylcholinesterase–new roles for an old actor. Nat. Rev. Neurosci. *2*, 294–302.

Straub, V., and Campbell, K. P. (1997). Muscular dystrophies and the dystrophin-glycoprotein complex. Curr. Opin. Neurol. *10*, 168–175.

Turney, S. G., Culican, S. M., and Lichtman, J. W. (1996). A quantitative fluorescence-imaging technique for studying acetylcholine receptor turnover at neuromuscular junctions in living animals. J. Neurosci. Methods *64*, 199–208.

van Mier, P., and Lichtman, J. W. (1994). Regenerating muscle fibers induce directional sprouting from nearby nerve terminals: studies in living mice. J. Neurosci. *14*, 5672–5686.

Xie, W., Stribley, J. A., Chatonnet, A., Wilder, P. J., Rizzino, A., McComb, R. D., Taylor, P., Hinrichs, S. H., and Lockridge, O. (2000). Postnatal developmental delay and supersensitivity to organophosphate in gene-targeted mice lacking acetylcholinesterase. J. Pharmacol. Exp. Ther. *293*, 896–902.

Ziskind-Conhaim, L., Geffen, I., and Hall, Z. W. (1984). Redistribution of acetylcholine receptors on developing rat myotubes. J. Neurosci. *4*, 2346–2349.